Proc. Natl. Acad. Sci. USA
Vol. 93, pp. 11956–11961, October 1996
Neurobiology

A model of multiplicative neural responses in parietal cortex

EMILIO SALINAS AND L. F. ABBOTT

Volen Center for Complex Systems, Brandeis University, Waltham, MA 02254-9110

Communicated by Nancy Kopell, Cambridge, MA, July 29, 1996 (received for review May 7, 1996)

ABSTRACT **Visual responses of neurons in parietal area 7a are modulated by a combined eye and head position signal in a multiplicative manner. Neurons with multiplicative responses can act as powerful computational elements in neural networks. In the case of parietal cortex, multiplicative gain modulation appears to play a crucial role in the transformation of object locations from retinal to body-centered coordinates. It has proven difficult to uncover single-neuron mechanisms that account for neuronal multiplication. Here we show that multiplicative responses can arise in a network model through population effects. Specifically, neurons in a recurrently connected network with excitatory connections between similarly tuned neurons and inhibitory connections between differently tuned neurons can perform a product operation on additive synaptic inputs. The results suggest that parietal responses may be based on this architecture.**

Responses of neurons in parietal area 7a, like those of other visual cells, are tuned to the location of visual images on the retina. In addition, area 7a neurons are strongly modulated by eye and head position, exhibiting a gain field that depends on the direction of gaze (1–4). Gain fields appear to be approximately linear functions of gaze direction (2, 3, 5), although they may saturate at low and high gain (6, 7). Gain modulation modifies the amplitude of the neural responses but does not change the preferred retinal location of a cell (the retinal location where a spot of light produces the maximal response) nor, in general, the width of the receptive field. Gain-modulated responses can be fit by a product of two functions, one that depends only on the retinal location of the visual stimulus and describes the receptive field, and another that depends only on gaze direction and accounts for the gain field. As a result, these cells produce a representation that is a product of their two types of input (3). Other cases of neurons that form multiplicative representations have also been reported, including examples from the insect visual system (8), area LIP (3), and the superior colliculus (9).

Neurons with multiplicative responses are extremely powerful computational elements in neural networks. This has been shown for abstract model neurons known as Σ-Π units (10–12) and for more biologically motivated models (5–7, 13, 14). The case of parietal responses is particularly interesting because their multiplicative behavior appears to provide an extremely useful intermediate representation of the location of targets for motor actions. This representation allows visual information about target location in retinal coordinates to be transformed to body-centered coordinates useful for guiding reaching movements (5–7, 13, 15).

It has proven extremely difficult to develop plausible mechanisms that allow single neurons to perform a product operation on their inputs (11, 12, 16, 17). Here we will show that, in contrast, recurrently connected populations of model neurons can produce multiplicative responses even when the individual cells sum their synaptic inputs linearly and are not intrinsically capable of computing a product. The multiplicative neuronal responses seen in the model are thus an emergent property of the network, not of its individual elements.

The model we use represents the neurons and synaptic connections within a patch of parietal cortical tissue. Recurrent connections are adjusted so that units with overlapping visual receptive fields excite each other, whereas those with nearby but separated receptive fields have inhibitory interactions. This is a common feature of recurrently connected cortical models (18–22). In areas of cortex where a retinotopic organization exists, this is equivalent to having excitation between cells that are near each other and inhibition between cells that are further apart, but this pattern of synaptic connectivity does not require a topographical architecture. In addition to recurrent connections, each cell receives inputs representing the afferent retinal and gaze-direction signals. Although we will illustrate and discuss briefly how the model can suppress noise, select between multiple inputs, and exhibit short-term memory, we will focus primarily on its ability to produce multiplicative responses.

Cortical models similar to the one used here have been studied previously and found to exhibit a number of interesting dynamical features. Ben-Yishai *et al.* (18) noted that models of this type can develop fixed line attractors (rather than fixed points) and thus can generate a stereotyped peak of activity across the neural population even for a uniform input. Both Ben-Yishai *et al.* (18) and Somers *et al.* (19) used networks with this structure to model the orientation tuning of neurons in primary visual cortex (V1). They observed that the orientation selectivity of the model neurons, like that of V1 neurons, does not broaden as a function of increased contrast. This contrast constancy is related to the multiplicative property that we uncover here. Douglas *et al.* (20) applied a related model to simulate motion tuning of cortical cells and observed that the recurrent architecture acted to reduce input noise. Stemmler *et al.* (21) used a similar model to study the effects of visual stimuli outside the classical receptive field.

The Network Model

The network model we study is constructed from individual model neurons that mimic the responses of parietal neurons to spots of light in different locations within the visual field. We do not model all of the multiplicative cells in area 7a, but rather a subset having similar gain-field properties. Furthermore, to reduce the number of neurons in the model, we consider a simplified situation where the location of the visual stimulus has a variable horizontal position but is held fixed in the vertical direction. Gaze direction will be similarly constrained to one dimension. This simplification has the added benefit of allowing the full network activity to be visualized. The reduction to one dimension is only a matter of convenience; the model can readily be extended to include the full two-dimensional visual field.

Neurons in the model are driven by inputs representing afferents that carry information about the retinal location of the visual stimulus and about the direction of gaze. The magnitude of the visual input to each cell depends on the distance between the location of the visual stimulus and the preferred retinal location for that cell. Across the population,

The publication costs of this article were defrayed in part by page charge payment. This article must therefore be hereby marked "*advertisement*" in accordance with 18 U.S.C. §1734 solely to indicate this fact.

the preferred retinal locations span the full range of possible stimulus locations in the horizontal dimension. When the stimulus is at the preferred location the neuron fires at its maximum rate, and the firing rate decreases as a Gaussian function of retinal position as the stimulus moves away from the preferred location. The model neurons also receive an input that varies linearly as a function of gaze direction and is the same, or approximately the same, for all neurons. The retinal position and gaze-direction inputs are summed linearly by each model neuron.

In addition to the stimulus location and gaze-direction inputs, each neuron makes recurrent synaptic connections with other neurons in the network. The strength and sign of the recurrent synapses depend on the distance between the preferred retinal locations of the pre- and postsynaptic neurons. The synaptic strength is positive if the two preferred locations are near to each other, becomes negative for larger separations, and ultimately goes to zero. Positive strengths correspond to excitatory synapses and negative ones to inhibitory synapses. Rather than dividing the model neurons into excitatory and inhibitory subpopulations, we allow individual units to make both excitatory and inhibitory connections. Thus, each network element is effectively an average or composite "neuron" representing an ensemble of both excitatory and inhibitory cells. This simplification, equivalent to a mean-field approximation, can be justified for large neuronal populations (18). Furthermore, the behavior of the network can be reproduced nearly identically using a network of separate inhibitory and excitatory units.

The input to cell i in the network arising from sources external to the network is the sum of two terms: a visual afferent input h_i^V and a gaze-direction afferent h_i^G. The location of the visual stimulus (in retinal coordinates) is represented by the variable x and the gaze direction (the location of the fixation point) is denoted by y. Both of these variables can take positive and negative values, corresponding to retinal locations to the right and to the left of the fixation point, or gaze directions to the right and left of the midline, respectively. Thus, $x = 0$ is the fixation point and $y = 0$ corresponds to a straightforward gaze relative to the body. In terms of these afferent contributions, the total external input to neuron i, denoted by h_i, is

$$h_i = h_i^V(x) + h_i^G(y). \qquad [2.1]$$

Note that in this expression the retinal and gaze-direction terms are additive. In the following, we refer to h_i as the external input or sometimes simply as the input to the neuron.

The visual input to neuron i takes its maximum value h_{max}^V when $x = x_i$, where x_i is the preferred retinal location for that cell. For other stimulus locations, the external input to each neuron is a Gaussian function of the difference between the stimulus location on the retina and its preferred location, with a width of $2\sigma_V$,

$$h_i^V(x) = h_{max}^V \exp\left(-\frac{(x - x_i)^2}{2\sigma_V^2}\right). \qquad [2.2]$$

The visual input to each cell is different due to the difference in preferred locations x_i. In contrast, the input representing gaze direction is similar for all cells and it increases or decreases linearly as the gaze direction changes,

$$h_i^G(y) = m y_i + b_i. \qquad [2.3]$$

The parameters m_i and b_i are the slope and offset of the gaze-direction signal. All offsets will be taken to be positive. These two parameters will either be the same for all cells, in which case we refer to them as m and b, or will be chosen from Gaussian distributions with fixed means and standard deviations.

The firing rate of neuron i is also affected by recurrent synapses through an additional recurrent input $\Sigma_j W_{ij} r_j$. Here r_j is the firing rate of neuron j in the network, and we have assumed that the recurrent input to neuron i from any other neuron j is equal to the product of the firing rate of neuron j times the synaptic weight factor W_{ij}. The recurrent synaptic connections between neurons depend on the distance between their preferred retinal locations. The synaptic weight W_{ij} from presynaptic neuron j to postsynaptic neuron i is given by a difference of two Gaussians

$$W_{ij} = A_E \exp\left(-\frac{(x_i - x_j)^2}{2\sigma_E^2}\right) - A_I \exp\left(-\frac{(x_i - x_j)^2}{2\sigma_I^2}\right), \qquad [2.4]$$

where $A_E > A_I$ and $\sigma_I > \sigma_E$. The network can be extended to include separate excitatory and inhibitory neurons by separating these two terms between two subpopulations.

When the sum of the external input and the recurrent contribution to a neuron is less than a threshold value h_{th}, the neuron is silent. For larger inputs, we assume the firing rate increases linearly. As a result, the firing rate of neuron i in response to the input h_i is given by the equation

$$r_i = s\left[h_i + \sum_j W_{ij} r_j - h_{th}\right]_+, \qquad [2.5]$$

where the expression $[x]_+$ is equal to 0 if $x < 0$ and is equal to x otherwise. For simplicity we set the threshold, h_{th}, and the slope of the firing-rate function, s, to be the same for all cells. We could include a rate-limiting term in the firing-rate function, but we work in a regime where this is unnecessary. For convenience, s is chosen so that the firing rates in our simulations lie in the range $0 \le r \le 1$ and thus all firing rates are expressed as fractions of a maximum rate.

For the simulation shown in Fig. 1, and for other simulations discussed but not shown here, we added a noise term to the input for each cell. The noise was random and uncorrelated between cells. Its value was chosen from a Gaussian distribution with standard deviation equal to the mean value of the external input h_i.

Results

Noise Suppression. One of the advantages of recurrent connectivity is that it effectively suppresses input noise (20). This is illustrated in Fig. 1, where mean network inputs and responses are plotted along with error bars representing their standard deviations. In all cases studied, the variability in the responses was smaller than that of the inputs by at least an order of magnitude. Although these results did not include the effects of noise generated internally within the network, the ability to reduce uncorrelated input noise is impressive. We show this figure in part because, for clarity, noise effects will not be included in subsequent figures. In all cases, when the effects of noise were included, the results were similar to those seen in Fig. 1.

Another interesting feature of the responses in Fig. 1 is that the activity profile is narrower than the input signal (notice the different scales for the x-axes in Fig. 1 *A* and *B*). This occurs because the recurrent excitation amplifies small asymmetries in the input (18–20).

Multiplicative Gain Fields. Our simulations reveal that when recurrent synaptic coupling is present, the gaze-direction signal acts as a gain factor that multiplies the retinal location-dependent responses. We illustrate this first for a network of neurons with identical gaze-direction slope and offset parameters m and b. With $m > 0$, this corresponds to all cells having gain fields that increase to the right. Fig. 2*A* shows the responses of a neuron in the network as a function of the

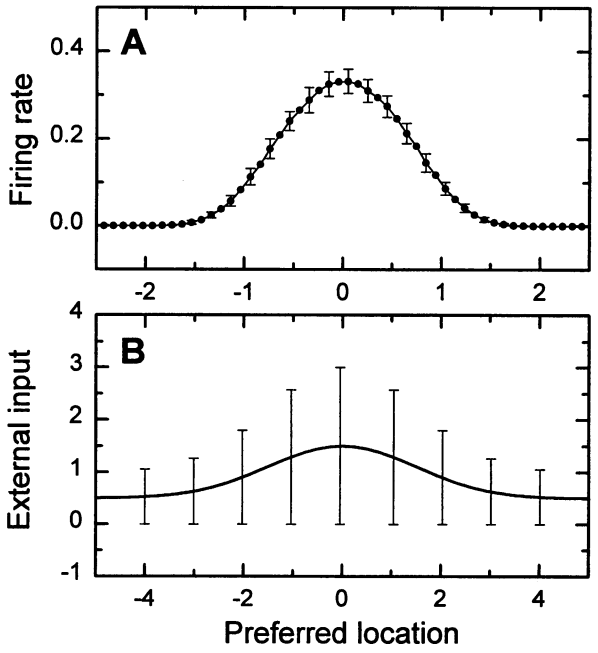

FIG. 1. Network responses in the presence of high input noise. (*A*) Firing rates of the cells plotted against their preferred retinal locations. Each dot represents a separate neuron. One hundred cells were used with preferred locations in the range $(-5, 5)$ (in arbitrary units). In all figures firing rates are expressed as fractions of a maximum rate. Dots represent the mean responses and error bars show the standard deviations of these responses. The line joining the dots is drawn to guide the eye. For clarity, error bars are shown only for every other cell. (*B*) Inputs for all cells plotted as a function of their preferred retinal locations. The plotted input is h_i, as defined in Eq. **2.1**. All inputs had standard deviations equal to the mean but, to avoid crowding, error bars are shown only for a few locations. Values for the inputs were selected from a Gaussian distribution. The standard deviations in the firing rates are more than an order of magnitude smaller than those of the inputs. Note the different scales for the horizontal axes in *A* and *B*. Parameters used were as follows: $s = 0.2$, $h_{\text{th}} = 1$, $m = 1$, $b = 0.5$, $h^V_{max} = 1$, $\sigma_V = 1.5$, $\sigma_E = 1$, $\sigma_I = 10$, $A_E = 10.5$, $A_I = 7.0$. For this figure the gaze direction was fixed at $y = 0$.

location of the visual stimulus for different values of the gaze direction y. Because the equations and their solutions are translation-invariant, all neurons exhibit response tuning curves with the same shape and gain field, but the responses are shifted to different preferred retinal locations for different cells. In terms of the parameters used by Andersen *et al.* (3), all of the units have the same gain-field slope and intercept. In Fig. 2*A*, unit responses are plotted as lines. The inputs to the cell are shown in Fig. 2*B*. From this panel it is clear that the linear gaze-direction input acts simply as an additive constant "base" on top of which rides the Gaussian retinal position signal. To illustrate the multiplicative nature of the responses, squares were drawn in Fig. 2*A* by multiplying the response corresponding to fixating straight ahead (the line without squares) by a fixed factor for each gaze direction. These factors were chosen to match the peak responses. The excellent agreement between the squares and the lines in Fig. 2*A* shows that the neural responses are accurately multiplicative. A stereotyped visual response is multiplied by a linear function of the gaze direction.

As a comparison, we studied whether two different feedforward networks could produce multiplicative outputs. In both cases, no recurrent connections were involved. In the first model, the neurons subtracted a threshold from their external inputs and then scaled and rectified the result to produce firing rates. This corresponds to turning off the recurrent connections in the original model. The factor s was adjusted so that the responses had about the same magnitude as those in Fig. 2*A*. The result is shown in Fig. 2*C*. Although both the visual and gaze-direction inputs affect the response, it is not in the form of a product; instead, the responses are essentially chopped versions of the input. For higher values of gaze input the tuning curves broaden, and at the highest value the neuron fires in response to stimuli at all retinal locations. In viewing Fig. 2 it is helpful to note that the threshold is equal to one and, thus, that the effective inputs to the network are those above this value.

The second feedforward network considered had units with sigmoidal functions describing the dependence of the firing rate on the external input,

$$r_i = \frac{r_{max}}{1 + \exp(c(h_{th} - h_i))}, \qquad [3.1]$$

where c is a constant. This is a form commonly used for the activation function of units in artificial neural networks (e.g., ref. 23) and it was used in this context to model parietal responses (5). For this model, the tuning curves are approximately multiplicative when the gaze direction is close to zero, but there is considerable deviation from a truly multiplicative response for more lateral gaze directions. For example, the width of the tuning curves varies as a function of gaze direction (Fig. 2*D*). Thus, a purely feedforward network in which units have sigmoidal gain functions can only produce responses that are reasonably close to multiplicative when the gaze angle is small in amplitude.

Although it is conceivable that roughly multiplicative responses are generated by sigmoidal firing-rate curves, this seems rather unlikely for several reasons. First, the measured gain fields of some cells for gaze angles differing by more than 30 degrees seem to be almost perfectly multiplicative (see figure 2*A* in ref. 4). This represents a degree of accuracy in generating multiplicative responses that cannot be reproduced by the sigmoidal mechanism. Second, recurrent connections are ubiquitous throughout cortical tissue, suggesting that the firing of a given cortical neuron is affected strongly by the activity of its neighbors. Third, cortical neurons tend to have sharp firing thresholds that do not match the smooth rise in firing output implied by the sigmoidal curve. The recurrent connections also provide some additional capabilities that would seem desirable from a functional point of view. As we showed in the previous section, they produce responses that are very robust to input noise. In a network with a simple feedforward organization, input fluctuations are not similarly reduced.

Up to now we have assumed that all neurons in the model network receive the same gaze-direction signal characterized by identical parameters m and b. We now investigate how cell-to-cell variability in the gain-field parameters affects multiplicative network responses. We do this by choosing the gaze-direction slopes and offsets from Gaussian distributions with standard deviations equal to one-half their mean values (however, both quantities are required to remain positive). The results are shown in Fig. 3, where tuning curves from four representative cells out of 500 in the full network are plotted. The responses show some variability in their amplitudes and widths, but it is certainly not comparable to the large variability in the inputs. The responses are neither perfectly symmetric nor identical for all cells, as was to be expected from the fact that variability in m and b breaks translation invariance. The cell in Fig. 3*D* shows a non-multiplicative effect for negative gaze directions. A few other units in the network were observed with similar non-multiplicative components in their responses; however, for most cells the responses are quite close to being multiplicative. The cell-to-cell variability and deviations from multiplicative behavior depend on the number of cells in the network and both are reduced in larger networks.

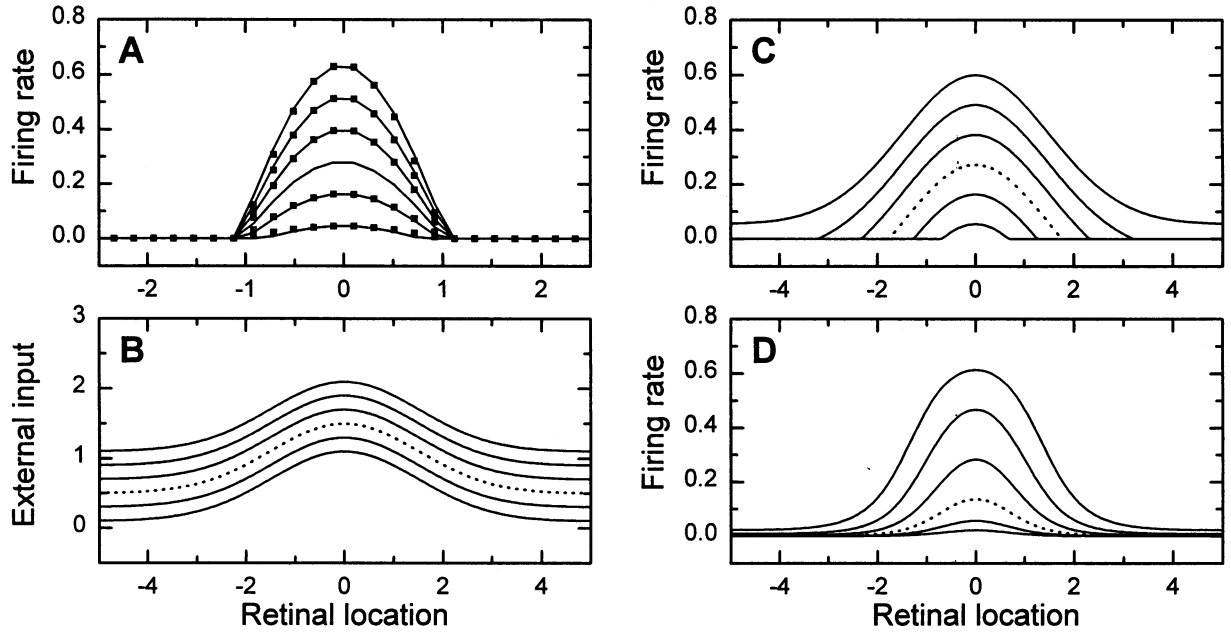

FIG. 2. (*A*) Gain-modulated receptive field of a single unit in a network of 500 cells. The *x*-axis indicates the location of the visual stimulus. Lines indicate the actual responses; squares were obtained by multiplying the middle curve (without squares) by different fixed factors. The different curves correspond to different gaze directions, with the middle one representing fixation straight ahead. Gaze direction modulates the amplitude of the visually evoked responses in an almost perfectly multiplicative way. Parameters in the model were as in Fig. 1. Gaze direction varied from −0.4 to 0.6 in steps of 0.2 (in arbitrary units), corresponding to curves from low to high amplitude. (*B*) The external input to the cell is shown for each stimulus location. The different curves correspond to different gaze directions. Note the scale in the *x*-axis as compared with *A*. (*C*) Response of a unit in a simple feedforward network equivalent to turning off the recurrent connections in the original model. The inputs were as in *B*. Parameters were as in *A*, except: $s = 0.6, A_E = 0, A_I = 0$. (*D*) Response of a unit in a second feedforward network to the same input shown in *B*. The units had sigmoidal activation functions given by Eq. **3.1**, with $r_{max} = 0.75, h_{th} = 1.8, c = 5$. The feedforward responses are not multiplicative. In *B–D*, the broken line indicates fixation straight ahead.

Additional Network Response Properties. The network we have analyzed exhibits a number of other interesting properties that, although not directly related to multiplicative responses, may be of interest and importance for visually guided reaching tasks. Visual areas encode information about many objects in a visual scene but typically only one of these acts as a reaching target at any given time. Therefore, at some stage in the sensory-motor pathway the visual representation has to be edited so that information about the non-targets is eventually filtered out (24). Our model network reveals a mechanism by which this selection process could take place. It is based on the network behavior that arises when two inputs, corresponding to two visual stimuli, are simultaneously presented. This is illustrated in Fig. 4, with firing rates plotted for the whole neuronal population. The two bell-shaped inputs in Fig. 4*B* represent two potential targets situated at different locations

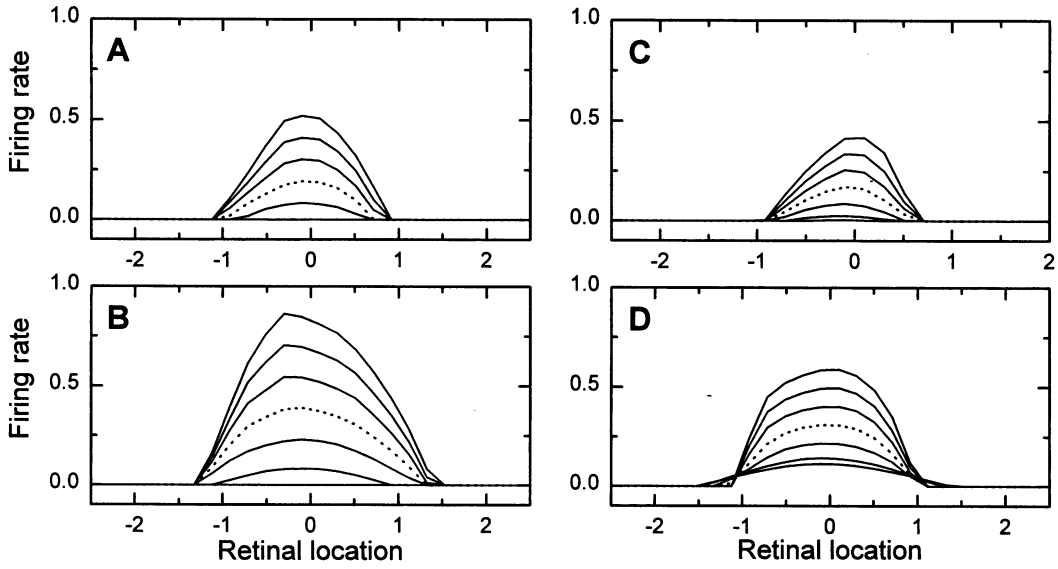

FIG. 3. Four representative gain-modulated responses from a network of 500 units in which parameters m_i and b_i were chosen from Gaussian distributions and thus varied from cell to cell. Standard deviations were equal to one-half the mean values, which were $m = 1$, and $b = 0.5$. Other parameters were as in Fig. 1. The different curves were obtained for different gaze directions with the broken lines indicating fixation straight ahead. There is some cell-to-cell variability in the gain fields, but the responses are close to multiplicative (compare with Fig. 2*A*).

in the visual field. The recurrent connections generate a nonlinear behavior producing a population response profile (Fig. 4*A*) with just a single peak matching the location of the strongest input. The strongest input is selected even if the peaks are very close to each other, as long as they are distinguishable as two separate peaks. They can also be far apart, as long as the separation is within the range of inhibition determined by σ_I. The whole neural population participates in a network version of a winner-take-all competition (23) in which the location of the strongest input is selected. A similar mechanism has been proposed as the basis for target selection during saccadic eye movements (25, 26).

Given that the strongest input selection mode of the model is based on the difference in strengths between simultaneously presented signals, the question arises as to how these signals might be internally biased. It is conceivable that modulatory effects like those described for attention (27–29) might first enhance one or another of the inputs simultaneously present, so that it becomes the winner in a downstream representation. This selection process could take place somewhere else in the sensory-to-motor pathway outside parietal area 7a. Such a mechanism would cause the responses to two stimuli presented simultaneously to resemble those evoked by a single stimulus.

Up until now, we have generally considered cases in which the constant baseline input b is below threshold. If the baseline excitatory input rises above the input threshold a qualitatively different behavior appears, as discussed by Ben-Yishai *et al.* (18). When the visual input is removed, the network activity diminishes somewhat but persists locked at the location where the visual stimulus was formerly located. Activity in this self-sustaining regime is quite robust; it will stay fixed in the same position even in the presence of other inputs at different locations. It is also robust with respect to noise in the inputs, although variation across cells does tend to shift the activity peak. The baseline needs to be reduced below threshold for the network to be silenced and reset. We will not elaborate on the implications of this type of behavior, but we note that with this self-sustained mode the neural network could act as a short-term memory buffer for target location information during a delay reaching task.

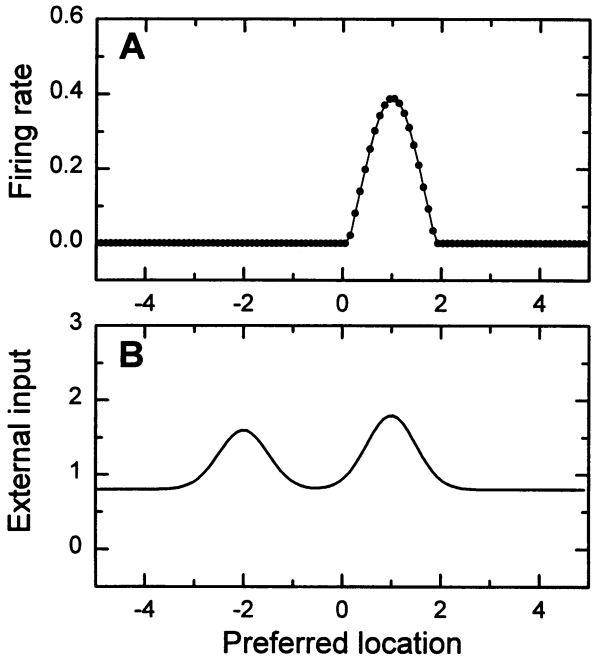

FIG. 4. Response of the model network when two visual stimuli are presented simultaneously at two different retinal locations. (*A*) The firing rates of all network cells are indicted by dots plotted at a position along the x-axis equal to their preferred retinal locations. A line is drawn through the dots to guide the eye. Only one peak of activity is generated in the network, matching the location of the strongest input. (*B*) The input evoking the activity in *A*. For this simulation 100 cells were used. The width of the inputs was lowered ($\sigma_V = 0.5$) so the two peaks could be clearly separated, and the offset was raised ($b = 0.8$) to increase the amplitude of the response. The rest of the parameters were as in Fig. 1, with $h^V_{max} = 0.8$ for the smaller input and $h^V_{max} = 1$ for the larger one. The gaze direction was $y = 0$.

Discussion

Strong recurrent synaptic connections in a neural network tend to produce stereotyped responses because population activity is primarily controlled by recurrent connections that do not depend on the stimulus. In such a network, the afferent, stimulus-dependent inputs serve to choose between a number of possible stereotyped responses. The recurrent network model we used has potential response profiles centered at any retinal location because it was constructed in a translationally invariant manner. Furthermore, the activity profiles come in families of different amplitudes but similar shapes, i.e., profiles that are related by multiplicative factors. The role of the afferent inputs in the model is to choose among these possible responses. The visual input that depends on the location of the stimulus breaks the translational invariance and determines which of the shifted activity profiles appears. The gaze-direction input is translationally invariant, being identical or similar for all neurons. Thus, it does not determine the location of the population response but rather fixes its amplitude by selecting from the multiplicative family of possible responses. The net result of the interaction between the two inputs is a response that signals the location of the stimulus in retinal coordinates and that is multiplied by a gaze-direction-dependent factor. This is exactly as observed in the gain-modulated responses of parietal neurons; thus, our model describes a functional building block for parietal cortex. All of the neurons in our model had similar gain-field properties because we modeled only a subset of parietal neurons receiving similar gaze-direction afferents. Describing cells in area 7a with different gaze-direction responses would require including a number of similar populations with different afferent dependencies.

The multiplicative combination of inputs produced by the model is quite robust; minor variants of the results shown in Fig. 2*A* can be obtained within a large range of parameter values. For example, reducing the strength of the excitatory connections to $A_E = 8.0$ lowers the response amplitudes for all gaze angles, but does not disrupt the multiplicative character of the gain modulation. Further reducing A_E does disrupt the effect, but this happens when it falls below the strength of the inhibitory connections, A_I, in which case there is no excitation. Similarly, modifying the connection ranges, for example setting $\sigma_I = 3.0$, affects the shape of the tuning curves (and might alter the responses to two simultaneously presented inputs) but leaves the multiplication intact. An important factor determining whether or not a multiplicative interaction is generated is the width of the input signal relative to the range of the excitatory connections. A multiplicative behavior is produced robustly whenever $\sigma_V \geq \sigma_E$, but fails when narrower inputs are used.

Although we applied the model to parietal neurons, nothing restricts its application exclusively to this case. Because the gaze-direction input was a linear function in the model, the multiplicative gain fields that resulted were linear. However, it should be stressed that the linear nature of the gaze direction input is not an essential feature of the model. If the gaze-direction input was taken to be any other function of gaze direction, the resulting responses would still be multiplicative but the gain field would be a nonlinear function of y. In this way, gain fields with arbitrary functional dependencies can be generated. The key feature that produced multiplicative re-

sponses was the fact that one input (the visual one) was distinct for each neuron, whereas the other (the gaze-direction input) was similar for each neuron. This generality raises the possibility that recurrent architectures could be used to model gain fields in other systems such as the superior colliculus (9), and for other modalities such as attention (27–29).

Parietal cells project to many other motor areas (30). Presumably these play different functional roles in motor control, so they may need to extract different pieces of information from the same input. Previous studies (5–7, 13) suggest that the multiplicative parietal representation of target location and gaze direction may be constructed precisely to fulfill this requirement. The multiplicative character of the neural responses produces a versatile information pool from which downstream circuits can read out various linear combinations that are relevant for their function (13). The utility and power of multiplicative representations in this system suggest that they may appear in other applications as well.

Research was supported by National Science Foundation Grant NSF-DMS9503261, the W.M. Keck Foundation, the Sloan Foundation, and the Conacyt–Fulbright–IIE program (E.S.).

1. Andersen, R. A. & Mountcastle, V. B. (1983) *J. Neurosci.* **3,** 532–548.
2. Andersen, R. A., Essick, G. K. & Siegel, R. M. (1985) *Science* **230,** 450–458.
3. Andersen, R. A., Bracewell, R. M., Barash, S., Gnadt, J. W. & Fogassi, L. (1990) *J. Neurosci.* **10,** 1176–1198.
4. Brotchie, P. R., Andersen, R. A., Snyder, L. H. & Goodman, S. J. (1995) *Nature (London)* **375,** 232–235.
5. Zipser, D. & Andersen, R. A. (1988) *Nature (London)* **331,** 140–143.
6. Pouget, A. & Sejnowski, T. J. (1995) in *Advances in Neural Information Processing Systems 7,* eds. Tesauro, G., Touretzky, D. S. & Lean, T. K. (MIT Press, Cambridge, MA).
7. Pouget, A. & Sejnowski, T. J. (1996) *J. Cognit. Neurosci.*, in press.
8. Hatsopoulos, N., Gabbiani, F. & Laurent, G. (1995) *Science* **270,** 1000–1003.
9. Van Opstal, A. J., Hepp, K., Suzuki, Y. & Henn, V. (1995) *J. Neurophysiol.* **74,** 1593–1610.
10. Rumelhart, D. E., Hinton, G. E. & McClelland, J. L. (1986) in *Parallel Distributed Processing: Explorations in the Microstructure of Cognition*, eds. Rumelhart, D. E., Hinton, G. E. & McClelland, J. L. (Wiley, New York), Vol. 1, pp. 605–636.
11. Mel, B. W. (1992) *Neural Comput.* **4,** 502–517.
12. Mel, B. W. & Koch, C. (1990) in *Advances in Neural Information Processing Systems*, ed. Touretzky, D. S. (Morgan Kaufmann, San Mateo, CA), Vol. 2, pp. 474–481.
13. Salinas, E. & Abbott, L. F. (1995) *J. Neurosci.* **15,** 6461–6474.
14. Pouget, A. & Sejnowski, T. J. (1994) *Cereb. Cortex* **4,** 314–329.
15. Andersen, R. A., Snyder, L. H., Li, C.-S. & Stricanne, B. (1993) *Curr. Opin. Biol.* **3,** 171–176.
16. Koch, C. & Poggio, T. (1992) in *Single Neuron Computation*, eds. McKenna, T., Davis, J. L. & Zornetzer, S. F. (Academic, Cambridge, MA), pp. 315–343.
17. Mel, B. W. (1993) *J. Neurophysiol.* **70,** 1086–1101.
18. Ben-Yishai, R., Lèv Bar-Or, R. & Sompolinsky, H. (1995) *Proc. Natl. Acad. Sci. USA* **92,** 3844–3848.
19. Somers, D. C., Nelson, S. B. & Sur, M. (1995) *J. Neurosci.* **15,** 5448–5465.
20. Douglas, R. J., Koch, C., Mahowald, M., Martin, K. A. C. & Suarez, H. H. (1995) *Science* **269,** 981–985.
21. Stemmler, M., Usher, M. & Niebur, E. (1995) *Science* **269,** 1877–1880.
22. Zhang, K. (1996) *J. Neurosci.* **16,** 2112–2126.
23. Hertz, J., Krogh, A. & Palmer, R. G. (1991) *Introduction to the Theory of Neural Computation* (Addison–Wesley, New York).
24. Maunsell, J. H. R. (1995) *Science* **270,** 764–769.
25. Kopecz, K. (1995) *Vision Res.* **35,** 2911–2925.
26. Kopecz, K. & Schöner, G. (1995) *Biol. Cybern.* **73,** 49–60.
27. Moran, J. & Desimone, R. (1985) *Science* **229,** 782–784.
28. Desimone, R. & Duncan, J. (1995) *Annu. Rev. Neurosci.* **18,** 193–222.
29. Connor, C. E., Preddie, D. C., Gallant, J. L. & Van Essen, D. C. (1996) *J. Neurophysiol.* **75,** 1306–1308.
30. Felleman, D. & Van Essen, D. C. (1991) *Cereb. Cortex* **1,** 1–47.